

Steady State Numerical Analysis of a Joule-Thomson Cryocooler for Cryosurgical Probe

R. V. Topkar¹ and M. D. Atrey¹

¹ Department of Mechanical Engineering, Indian Institute of Technology – Bombay, Mumbai – 400076

The Hampson-type Joule-Thomson cryocoolers are preferred for cryosurgical probes due to their small size and no moving parts. Due to substantial change of pressure and temperature both along both the inlet and returning streams, property variations of the working fluid and pressure drop in the streams have to be realistically accounted for. Numerical analysis is the key for such demanding design applications. In the present work, steady state simulation of the heat exchanger in the Joule- Thomson cryocooler is carried out numerically. The model predicts the pressure and temperature profiles of the high pressure inlet and low pressure returning stream. These results are validated using various data available in literature. Once validated, the steady state model is used for design of heat exchanger for Joule-Thomson cryocooler to be used in cryosurgical probe. Various key parameters of the heat exchanger that affect its performance are identified and their effect is studied.

Key words: Joule-Thomson Cryocooler, Cryosurgical Probe, Heat Exchanger, Steady-State Simulation, Temperature-dependent Properties

INTRODUCTION

A Joule-Thomson cryocooler is a closed system consisting of a heat exchanger, evaporator and an expansion device. A Joule-Thomson cryocooler is one of the most effective methods of providing low temperature cooling due to its features of short cool down time, compact size and no moving parts. The Hampson-type heat exchanger is usually used for this device mainly due to its space utilization. The heat exchanger consists of a helically coiled finned tube in an annulus between the inner mandrel and outer shield. The high pressure inlet fluid passes through the finned tube and is expanded by a Joule-Thomson expansion

process at the end. The expanded fluid produces cooling effect and delivers the same in the evaporator. This cold fluid at low pressure then, passes over the finned tube in the annular space precooling the incoming high pressure fluid. The working fluids normally used are nitrogen and argon.

The performance of the JT cryocooler is highly dependent on the effectiveness of the heat exchanger. Also, there is substantial change of pressure and temperature in the fluid on both sides of the heat exchanger and hence, property variations need to be taken into account while simulating the heat exchanger. Previous studies have been limited due to the complex geometry of the heat exchanger.

Ng et al. [1] and Xue et al. [2] reported the experimental and numerical study of the Joule-Thompson refrigerator for steady-state characteristics with argon as the working fluid. Numerical studies for transient characteristics of the Joule-Thompson refrigerator with nitrogen as working fluid using a one dimensional transient model are reported by Chien et al. [3] and Chou et al. [4]. Chua et al. [5] developed the geometry model of the Hampson-type cryocooler. Hong et al. [6] applied the effectiveness-NTU approach to predict the characteristics of a Joule-Thompson cryocooler for argon and nitrogen gas. Ardhapurkar and Atrey [7] identified an area correction factor to calculate the actual area of heat transfer on the cold side. Fredrickson [8] has modeled the cryosurgical probe consisting of a Joule-Thomson cryocooler and presented a study on the ice ball model. The model aims at maximizing the size of the ice ball produced at the tip of the cryosurgical probe.

In the present study, steady state numerical simulation of the heat exchanger in the Joule-Thomson cryocooler is carried out. The model predicts the pressure and temperature profiles of the high pressure and low pressure streams along the length of the heat exchanger. The steady state model is used for design of heat exchanger for Joule-Thomson cryocooler for a cryosurgical probe. The effect of various key parameters of the heat exchanger are then studied.

NUMERICAL MODEL

The one-dimensional model given by Ng et al. [1] is used for simulating the heat exchanger. The following assumptions are made for simulating the heat exchanger:

1. Temperature varies only along the length of the pipe (x-direction only).
2. There is no conduction in the fluid.
3. The emissivity of the surface of the shield is independent of temperature.

For implementing the one-dimensional model, accurate calculation of the heat transfer surface areas is required. The cross-sectional

area of the heat exchanger is considered for calculation of perimeters and areas of heat transfer between different components of the heat exchanger. Figure 1 shows the cross-sectional area of the heat exchanger.

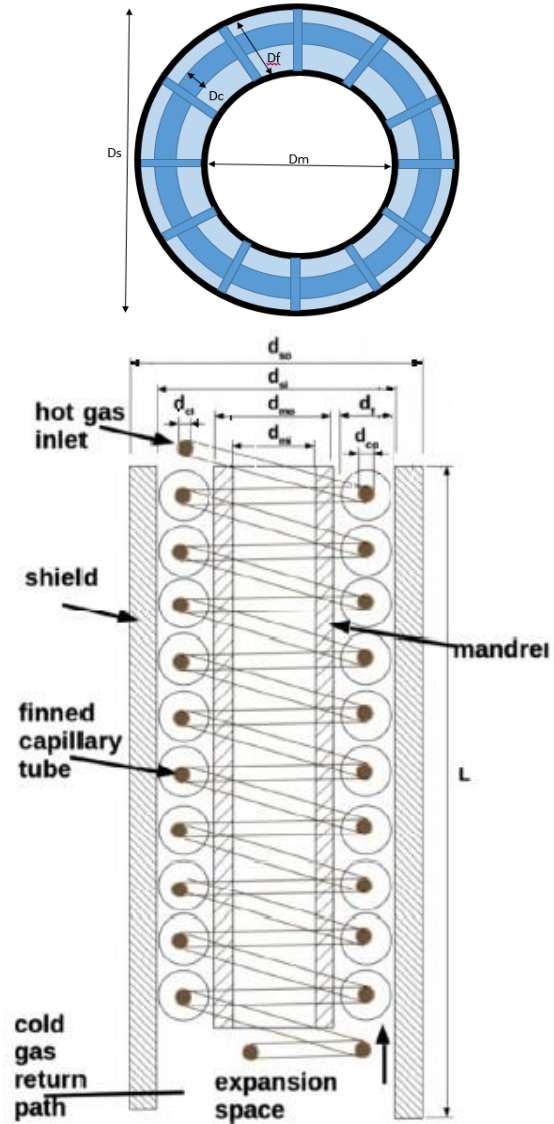


Figure 1. Cross-sectional View of the Heat Exchanger [7]

The flow area for the low pressure side is the area in the annular space without the finned tube and is given in Equation 1.

$$A_c = \pi(D_{si}^2 - D_{mo}^2 - (D_{hel} + D_{co})^2 + (D_{hel} - D_{co})^2) / 4 - \pi D_{hel} N t_{fin} (D_{fin} - D_{co}) \quad (1)$$

Similarly, the perimeter of the outer area of finned tube is calculated and given in equation 2.

$$P_{co} = \frac{\pi(\pi D_{hel})(N(D_{fin}^2 - D_{co}^2)/2 + D_{co}(1 - Nt_{fin}))}{Pitch} \quad (2)$$

The hydraulic diameter is used for the calculation of parameters associated with the return fluid stream. The area correction factor of 0.3 as given by Ardhapurkar et al. [7] is applied to account for the actual heat transfer area on the cold side. This accounts for the non-uniform flow distribution over the fin surface.

Thermophysical Properties

The MBWR equation of state given by Younglove [9] is utilized for getting the density given the pressure and temperature. The equation is non-linear and the bisection method is used for solving the equation. The thermal conductivity and viscosity are functions of density and temperature and are given by Hanley et al. [10]. The deviations in the thermophysical properties calculated using these equations is around a maximum of 0.5% which may lead to small errors in the calculated temperature and pressure profiles compared to actual thermophysical properties.

Governing Equations

The governing equations used for the model are given below.
Continuity Equation:

$$\frac{dm}{dx} = 0 \quad (3)$$

Momentum Equation:

$$\frac{dP}{dx} = -\frac{2fG^2}{\rho D} - G^2 \frac{d(1/\rho)}{dx} \quad (4)$$

Energy Equations for the hot fluid, cold fluid, tube, mandrel, and shield [Equations 5-9] respectively:

$$\dot{m}_h C_{ph} \frac{dT_h}{dx} = h_h p_{ci} (T_h - T_w) \quad (5)$$

$$\dot{m}_c C_{pc} \frac{dT_c}{dx} = h_c [p_{co} (T_c - T_w) + p_{si} (T_c - T_s) + p_{mo} (T_c - T_m)] \quad (6)$$

$$k_w A_w \frac{d^2 T_w}{dx^2} = h_h p_{ci} (T_w - T_h) + h_c p_{co} (T_w - T_c) \quad (7)$$

$$k_m A_m \frac{d^2 T_m}{dx^2} = h_c p_{mo} (T_m - T_c) \quad (8)$$

$$k_s A_s \frac{d^2 T_s}{dx^2} = h_c p_{si} (T_s - T_c) + h_r p_{co} (T_s^4 - T_{amb}^4) \quad (9)$$

The Fanning friction factor f for flow in a helical coil is given by:

$$f = 0.184(1 + 3.5 \frac{D_{ci}}{D_{hel}}) Re^{-0.2}$$

The convective heat transfer coefficients for flow given by Flynn [11] are employed in the model. They are as follows:

$$h_h = 0.023 C_{ph} G_h Re_h^{-0.2} Pr_h^{-2/3} (1 + 3.5 \frac{D_{ci}}{D_{hel}})$$

$$h_c = 0.26 C_{pc} G_c Re_c^{-0.4} Pr_c^{-2/3}$$

Where h_h is valid single phase turbulent flow with $Re > 10^4$ and h_c is valid for turbulent flow within the range of $2000 < Re < 3.2 \times 10^4$.

Boundary Conditions

The adiabatic boundary condition are applied at the ends of the tube for the shield, mandrel and tube. The inlet pressure and temperature for the hot fluid as well as for the cold fluid, after the evaporator, are defined.

The governing equations [Equations 3-9] are solved along with the boundary conditions by discretizing the length L of the heat exchanger using the finite difference method. The discretized equations are solved using the iterative Gauss-Seidel method. For this, an initial guess for the temperature and pressure at the nodes is made and the code is run till convergence of these parameters as

well as the properties. The thermophysical properties are updated at the start of each iteration using the previous pressure and temperature at that node.

Validation of the Model

The non-dimensional temperature (Equation 10) profiles obtained from the numerical simulation are compared with the profiles given by Ng et al. [1] and are shown in Figures 2 and 3.

$$\Theta(x/L) = \frac{T(x/L) - T_{c,in}}{T_{h,in} - T_{c,in}} \quad (10)$$

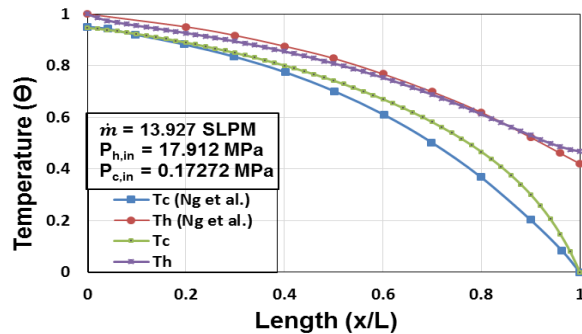


Figure 2. Temperature profiles ($P_{h,in}=17.912$ MPa)

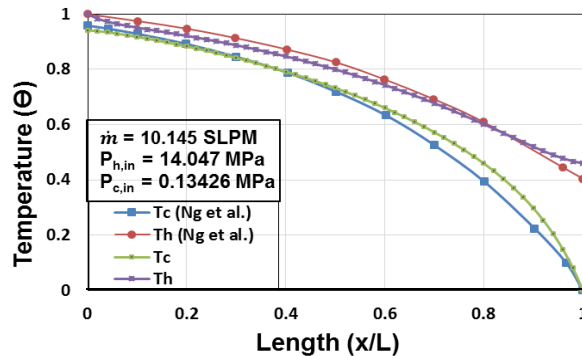


Figure 3. Temperature profiles ($P_{h,in}=14.047$ MPa)

As can be seen from the figures, the temperature profiles can accurately predict the cold end temperature to an error of 1%. The drop in pressure along the length of the heat exchanger is almost linear. The pressure drop in the inlet stream ΔP_h is compared with the experimental data and the results along with the temperature results at the cold fluid outlet are presented in Table 1. As can be seen, the pressure drop in the high pressure fluid is comparable to the experimental result. There is no experimental result available for the temperature profile in the heat exchanger. The error can be reduced by using more accurate thermophysical data.

DESIGN FOR CRYOSURGICAL PROBE

After the validation of the model, the design for using the heat exchanger for a Joule-Thompson cryocooler to be used as a cryosurgical probe is carried out. Instead of a finned tube, a capillary without fins is used for ease of winding around the mandrel and construction. Nitrogen is used as the working fluid for the non-finned tube due to ease of availability. The capillary is made from copper while the mandrel and shield are made from stainless steel. Parameters like the supply pressure, heat exchanger length, and helical diameter are considered. The high pressure fluid is expanded through an ideal isenthalpic process. The heat transfer coefficients are calculated for different Reynolds number as given by Flynn [11]. Temperatures considered are in the range of 100-150 K as required for a cryosurgical probe.

Table 1. Comparison of experimental and numerical data

Inlet Conditions				Ng et al. [1]	Numerical	Relative	Ng et al. [1]	Numerical
$P_{h,in}$	$P_{c,in}$	$T_{h,in}$	$T_{c,in}$	Experimental	$T_{c,out}$ (K)	Error	ΔP_h	ΔP_h
(MPa)	(MPa)	(K)	(K)	$T_{c,out}$ (K)		%	(MPa)	(MPa)
17.912	0.1727	291.49	110.36	282.57	282.95	0.134	10.926	10.23
16.968	0.1746	291.40	110.42	283.73	282.40	-0.469	-	
16.010	0.1636	292.25	109.90	284.77	282.18	-0.910	-	
14.966	0.1471	292.14	109.28	284.90	282.78	-0.74	-	
14.047	0.1342	291.94	108.70	284.98	282.64	-0.822	7.725	7.334

Effect of Supply Pressure

The effect of supply pressure is studied. Return line inlet pressure is kept constant at 1.5 bar and the length of heat exchanger is kept as 500 mm. Figure 4 shows the ideal cooling capacity at supply pressures from 60 to 100 bar.

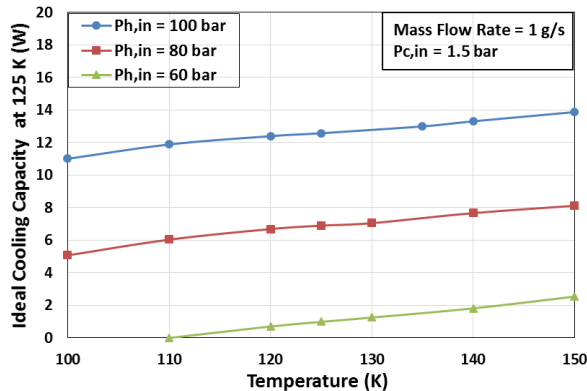


Figure 4. Ideal cooling capacity at different supply pressures

It can be seen that the increase in the supply pressure increases the ideal cooling capacity available at any temperature. A supply pressure of 100 bar results in a cooling capacity of 11 W at 100 K while with a supply pressure of 60 bar the lowest temperature achieved is around 110K.

Effect of heat exchanger length

The heat exchanger length is varied for a constant mass flow rate and the results are shown in Figure 5.

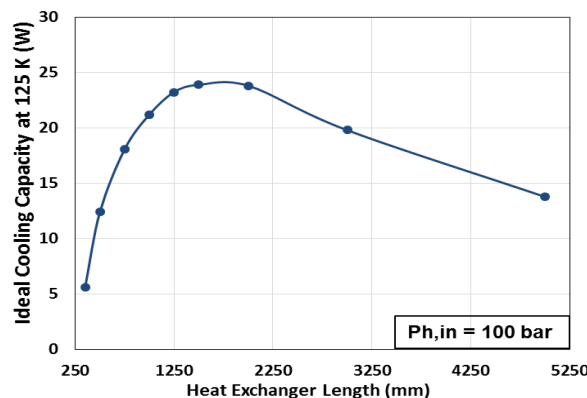


Figure 5. Effect of heat exchanger length on cooling capacity

The low pressure fluid outlet pressure is kept constant at 1 bar. As the heat exchanger length increases, the pressure drop along the length and the heat transfer area both increase. Also, the return stream inlet pressure also increases. Due to this, the ideal cooling capacity goes through a maximum as can be seen in Figure 5.

Effect of mass flow rate

The effect of mass flow rate on the ideal cooling capacity is studied for heat exchanger length of 500 mm and 750 mm. The study results are presented in Figure 6.

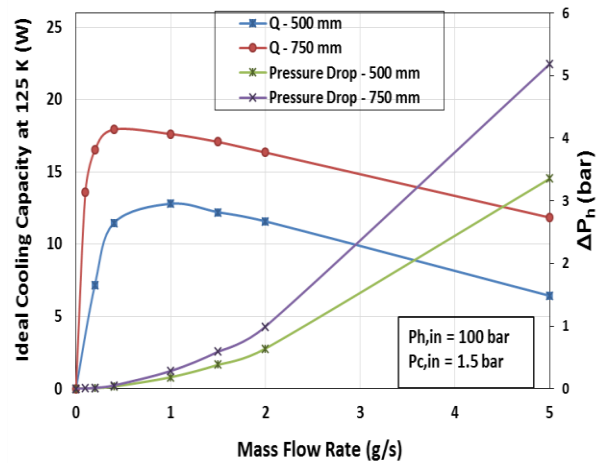


Figure 6. Effect of mass flow rate on cooling capacity

The pressure drop increases almost exponentially with an increase in mass flow rate. This results in an optimum cooling capacity for a given mass flow rate. The maximum cooling capacity occurs at lower mass flow rates for higher heat exchanger lengths.

Cryosurgical Probe

The above work is extended to design a cryosurgical probe for laboratory experimentation. The performance of the cryocooler is optimized to give sufficient cooling capacity at a low temperature. The design is carried out to yield a cooling capacity of 10 W at 125 K.

The maximum supply pressure is kept fixed at 10 MPa as a consideration for safety. The helical diameter and the heat exchanger

length are varied parametrically for minimum space utilization to lead to an optimum design. Finally, the mass flow rate is optimized for the above conditions. The cooling capacity at different temperatures for these optimized parameters is shown in Figure 8. The schematic of a cryosurgical probe is shown in Figure 9.

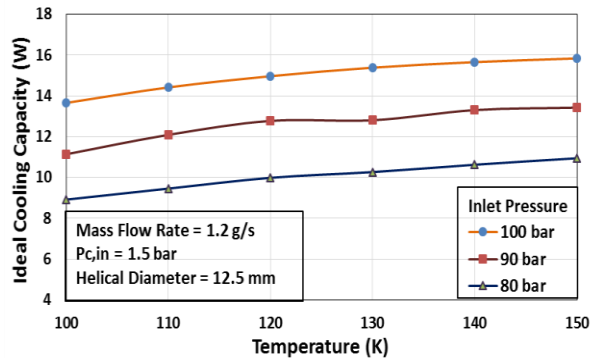


Figure 8. Ideal Cooling Capacity at different temperatures

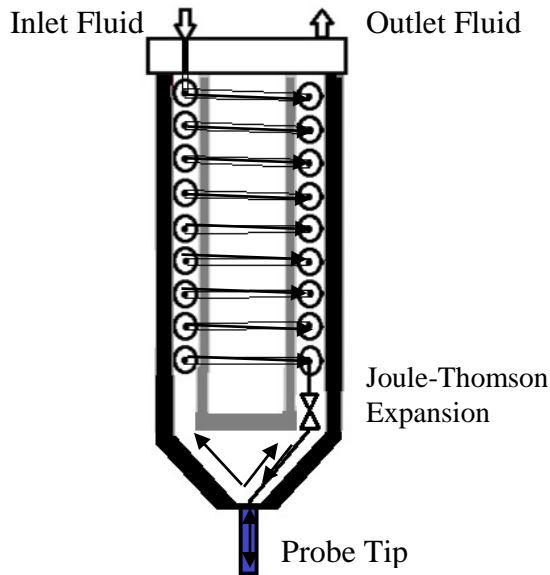


Figure 9. Schematic of Cryosurgical Probe

CONCLUSION

In the present work, the design for a cryosurgical probe is carried out using a numerical model that uses first-order discretization of the governing ordinary differential equations. The model takes into account the changes in thermo-physical

properties and the pressure drop. The variation of key parameters is studied and an optimized design is made. The fabrication of the probe is currently being carried out.

REFERENCES

1. Ng, K. C., Xue, H., and Wang, J. B., "Experimental and numerical study on a miniature Joule-Thomson cooler for steady-state characteristics," *Int. J. of Heat and Mass Transfer*, Vol. 45, pp. 609–618. (2002)
2. Xue, H., Ng, K.C., and Wang, J.B., "Performance evaluation of the recuperative heat exchanger in a miniature Joule-Thomson cooler," *Applied Thermal Engineering*, Vol. 21, pp.1829 -1844. (2001)
3. Chien, S. B., Chen, L. T., and Chou, F. C., "A study on the transient characteristics of a self-regulating Joule-Thomson cryocooler," *Cryogenics*, Vol. 36, pp. 979-984. (1996)
4. Chou, F. C., Pai, C. F., Chien, S. B., and Chen, J. S., "Preliminary experimental and numerical study of transient characteristics for a Joule-Thomson cryocooler," *Cryogenics*, Vol. 35, pp. 311-316. (1995)
5. Chua, H. T., Wang, X., and Teo, H. Y., "A Numerical study of the Hampson-type miniature Joule-Thomson cryocooler," *Int. J. of Heat and Mass Transfer*, vol. 49, pp. 582-593. (2006)
6. Hong, Y. J., Park, S. J., and Choi, Y. D., "A Numerical study on the performance of the miniature Joule-Thompson refrigerator," *AIP Conf. Proc.* 1218, 103 (2010)
7. Ardhapurkar, P.M., and M.D. Atrey., "Performance Optimization of a Miniature Joule–Thomson Cryocooler Using Numerical Model." *Cryogenics*, vol.63, pp.94-101. (2014)
8. Fredrickson, Kylie L. *Optimization of cryosurgical probes for cancer treatment*. Diss. University of Wisconsin - Madison, 2004.
9. Younglove, B., "Erratum: Thermophysical Properties of Fluids. I. Argon, Ethylene, Parahydrogen, Nitrogen, Nitrogen Trifluoride, and Oxygen". *J. Phys. Chem. Ref. Data*, 14(2), p.619. (1985)
10. Hanley, H., McCarty, R. and Haynes, W., "The Viscosity and Thermal Conductivity Coefficients for Dense Gaseous and Liquid Argon, Krypton, Xenon, Nitrogen, and Oxygen". *J. Phys. Chem. Ref. Data*, 3(4), p.979. (1974)
11. Flynn, T. M., *Cryogenic engineering*. New York: Marcel Dekker.(1997)